Climatic Change
DOI 10.1007/s10584-011-0376-2

Does global warming favour the occurrence of extreme floods in European Alps? First evidences from a NW Alps proglacial lake sediment record

B. Wilhelm · F. Arnaud · D. Enters · F. Allignol · A. Legaz · O. Magand · S. Revillon · C. Giguet-Covex · E. Malet

Received: 21 September 2009 / Accepted: 14 November 2011

Abstract Flood hazard is expected to increase in the context of global warming. However, long time-series of climate and gauge data at high-elevation are too sparse to assess reliably the rate of recurrence of such events in mountain areas. Here paleolimnological techniques were used to assess the evolution of frequency and magnitude of flash flood events in the North-western European Alps since the Little Ice Age (LIA). The aim was to document a possible effect of the post-19th century global warming on torrential floods frequency and magnitude. Altogether 56 flood deposits were detected from grain size and geochemical measurements performed on gravity cores taken in the proglacial Lake Blanc (2170 m a.s.l., Belledonne Massif, NW French Alps). The age model relies on radiometric dating (^{137}Cs and ^{241}Am), historic lead contamination and the correlation of major flood- and earthquake-triggered deposits, with recognized occurrences in historical written archives. The resulting flood calendar spans the last ca 270 years (AD 1740–AD 2007). The magnitude of flood

B. Wilhelm · F. Arnaud · F. Allignol · A. Legaz · C. Giguet-Covex · E. Malet
Laboratoire Environnement Dynamique et Territoire de Montagne, Le Bourget-du-Lac, France

D. Enters
Laboratoire Environnement Dynamique et Territoire de Montagne, Le Bourget-du-Lac, France

D. Enters
GEOPOLAR, Institute of Geography, University of Bremen, Bremen, Germany

O. Magand
Laboratoire de Glaciologie et de Géophysique de l'Environnement, Saint-Martin d'Hères, France

S. Revillon
Laboratoire Environnement Dynamique et Territoire de Montagne, Le Bourget-du-Lac, France

S. Revillon
IFREMER, Pouzané, France

B. Wilhelm (✉)
EDYTEM, Le Bourget-du-Lac, Campus Scientifique, Pôle Montagne, 73 376 Le Bourget-du-Lac, France
e-mail: bruno.wilhelm@univ-savoie.fr

Published online: 10 December 2011

events was inferred from the accumulated sediment mass per flood event and compared with reconstructed or homogenized datasets of precipitation, temperature and glacier variations. Whereas the decennial flood frequency seems to be independent of seasonal precipitation, a relationship with summer temperature fluctuations can be observed at decadal timescales. Most of the extreme flood events took place since the beginning of the 20th century with the strongest occurring in 2005. Our record thus suggests climate warming is favouring the occurrence of high magnitude torrential flood events in high-altitude catchments.

1 Introduction

Over last decades, noticeable climate changes have been observed at high elevation in European Alps. In-situ observations indicate an increase of the mean annual air temperature of 1°C to 2°C and a shift towards drier conditions, but with more intense precipitation events (Beniston et al. 1997; Frei and Schär 2001). However, most high-elevation areas are poorly monitored (Kieffer-Weisse and Bois 2001) and thus spatial and temporal datasets of mean and extreme precipitation rates are insufficient to reveal consistent trends. Furthermore, precipitation pattern and in particular extreme events are poorly simulated by climate models (Jasper et al. 2002; Beniston 2006; Frei et al. 2006) mainly due to complex topography effects. As a consequence, evidences of changes in extreme events pattern at high altitude remains sparse (Bronstert 2003). While an enhancement of severe flooding hazard is expected within the next decades due to an intensification of the hydrological cycle associated to global warming (Milly et al. 2002; Karl and Trenberth 2003; Huntington 2006), the question of current and future impact of climatic change on extreme events hence remains an open debate (Huntington 2006). Such issues present a particular public interest as tourism and recent demographic development in the Alps are increasing people and constructions vulnerability to natural hazards (Beniston and Stephenson 2004).

Floods are common and widespread natural hazards. They cause the loss of human life and high cost damage to property and infrastructure and are particularly destructive in mountain areas. For example, in August 2005 a series of catastrophic floods throughout the European Alps caused at least 40 deaths and several billion euros of damage, according to the international press.

To identify the effects of climate change on the frequency and magnitude of flood hazards, historical documents and gauge stations data provide valuable information (e.g. Benito et al. 2004). However, historic descriptions are by nature subjective. In particular, hazard perception by humans varied throughout time and descriptions of damages can thus be biased. Moreover, they may be fragmentary due to destruction or loss and they generally provide only a relatively short time span for analyses, especially in mountain areas. To overcome these limits, natural archives may be used as complementary records (Brazdil et al. 2005).

Among the various natural archives lake sediments have the advantage to be continuous records in which particular events are preserved such as flood events (Siegenthaler and Sturm 1991; Arnaud et al. 2002; Gilli et al. 2003; Bøe et al. 2006; Moreno et al. 2008), earthquakes (Chapron et al. 1999; Monecke et al. 2004; Nomade et al. 2005) or debris flows (Irmler et al. 2006). Using lake sediments, it is possible to construct flood calendars covering long-term periods (Nesje et al. 2001; Giguet-Covex et al. 2011) and to assess the magnitude of these events from the thickness or the mass of event-triggered deposits (Irmler et al. 2006; Nesje et al. 2001). In this study, we apply this approach to the sedimentary record of Lake Blanc (Belledonne Massif, NW French Alps). During flood events, coarser particles—coarse silt to fine sand—are carried to the deepest part of the lake where they form characteristic layers. The objective of this study is the reconstruction of a precise flood calendar in order to assess the evolution of frequency and magnitude of flood events at this high elevation environment in the context of global warming.

2 Study area and setting

2.1 Lake Blanc and its catchment

Lake Blanc (2170 ma.s.l., 45°10′42″N, 5°58′21″E) is located 5 km upstream the village of Sainte-Agnès in a small high-altitude cirque of 3 km² (Fig. 1). The geology is dominated by fractured metamorphic rocks (amphibolite and leptynite). Vegetation in the catchment is sparse, only the lower parts being covered by alpine meadows. Due to the high elevation (up to 2977 ma.s.l.) and a favourable orientation, the cirque hosts the Freydane Glacier, one of the last remaining ones in Belledonne Massif. Its evolution is well-marked in the landscape by a large proglacial area. In its uppermost part the bedrock appears beneath the currently retreating glacier. Downstream, a glacier-fed torrent forms a meandering zone (Fig. 1d). In the lowest part the slope increases and the torrent incises into the basal till and the largest and most distal moraine, attributed to the Little Ice Age (LIA) (Edouard 1994). The morainic material eroded and transported by the river originates essentially from the lowest part of the proglacial area (Fig. 1b). From November to May, the catchment area is

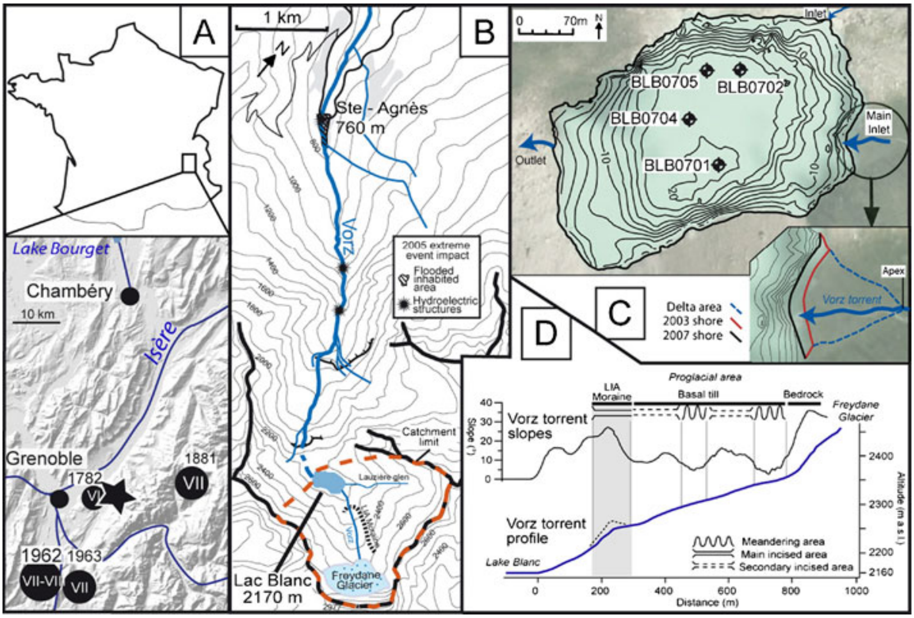

Fig. 1 Geographical setting of the study area and location of investigated lacustrine sediment archive. **a** Location of the study area (star) in the Belledonne Massif in French Alps and historical earthquakes (circles) with their respective dates and MSK intensities (roman numerals) (Lambert and Levret-Albaret 1996). **b** The main damages on the surrounding area of Sainte-Agnès triggered by the Vorz Torrent during the 2005 flood event and location of Lake Blanc catchment area (*red* and *dash line*) in the Vorz head catchment. The LIA moraine just upstream of Lake Blanc is indicated by a dotted line. **c** Bathymetry of Lake Blanc, location of the four studied sediment cores and zoom in the delta evolution in the right and low part. **d** Details of the Vorz Torrent characteristics (profile, slope and morphologies) in the Lake Blanc catchment

covered by snow and the lake is frozen, implicating a sediment input only during summer and early autumn. Lake waters remain turbid throughout this period indicating Lake Blanc receives a continuous input of glacial flour.

2.2 The 2005 extreme flood event of the vorz torrent

On August 21st to 23rd 2005 exceptional meteorological conditions (Grieser et al. 2005) resulted in numerous extreme flood events all over European Alps (Beniston 2006; Böhm and Wetzel 2006; Jaun et al. 2008). In French Alps, several villages located at the foothill of the Belledonne Massif (Fig. 1a) were affected (Prudent-Richard et al. 2008). In particular, in the village of Sainte-Agnès (760 m a.s.l.) the Vorz torrent caused more than 3.2 millions € estimated total damage with the destruction of three hydroelectric infrastructures, roads and bridges and the flooding of houses (Fig. 1b). This extreme event was triggered by intense precipitations reaching a total amount of 300 mm in two days in the highest part of the catchment area (Allignol et al. 2008).

3 Material and methods

3.1 Lake Blanc physical features and sediment cores

In summer 2007, a bathymetric survey was carried out at Lake Blanc and revealed a large subaquatic delta and a flat basin in the centre of the lake with a maximum water depth of 20.3 m. The bathymetric map compared with an aerial photo of 2003 showed also a delta progradation of 15 m (Fig. 1c). Four cores were retrieved from the deepest part of the lake, approximately in the prolongation of the delta (cores BLB0701 and BLB0704) and near the northern slope (cores BLB0702 and BLB0705).

In the laboratory, cores were split, photographed and a detailed description was made to determine the different lithofacies. BLB0704 was sampled following a 1-cm step and dried at 60°C during 4 days to obtain dry bulk density. Laser grain-size measurements were performed on cores BLB0701, BLB0702 and BLB0704 using a Malvern Mastersizer S following a sampling interval of 0.5 cm. Cross-plots of median grain size (Q50) and the coarse fraction assessed by the particle diameter at the 99-percentile (Q99) of the three facies were used to characterize the depositional processes (Passega 1964).

The grain-size data were supplemented by X-ray fluorescence (XRF) measurements performed on an Itrax™ core scanner at GEOPOLAR, University of Bremen (Germany) from core BLB0701 at 1-mm resolution. Relative concentration changes of Ca and Fe were used as a complementary approach of the classical grain size measurements to obtain a higher resolution. The use of the Ca/Fe ratio as a high-resolution grain size proxy is based on the assumption that Fe is mostly associated with fine particles (Cuven et al. 2010) whereas Ca is more abundant in coarser fractions.

Microstratigraphy was analyzed using impregnated thin sections from cores BLB0701 and BLB0704. For each core five 10-cm long slices were taken with a 2 cm overlap, shock-frozen, freeze-dried and impregnated with Araldite using methods described by Lotter and Lemcke (1999).

3.2 Chronology

In paleoenvironmental studies covering the last century, the age-depth model often relies on the use of ^{210}Pb and ^{137}Cs measurements. Such an approach is not sufficient in our case because the interpretation of ^{210}Pb profiles in high altitude terrigenous-dominated lake sediment is often complex (Arnaud et al. 2002). Moreover, in such a dynamic sedimentary environment considerable changes in sedimentation rates are expected. Consequently we used additional independent chronological markers in order to build up a reliable, high-resolution age-depth model.

^{137}Cs and ^{241}Am measurements were performed at the LGGE (Grenoble) on the upper 25 cm of core BLB0704 following a non-regular sampling step of approximately 1 cm, following facies boundaries. This allowed us to locate three chronostratigraphic markers: the fallout of ^{137}Cs from atmospheric nuclear weapon tests starting in the northern hemisphere in AD 1955 and culminating in AD 1963 as well as the fallout of ^{137}Cs owing to the Chernobyl accident in AD 1986 (Di Lauro et al. 2004). Only the nuclear weapon tests resulted also in a widespread fall-out of ^{241}Pu and the activity of its decay product, ^{241}Am, can now be measured in sediments (Appleby et al. 1991). The detection of ^{241}Am hence allows to identify the 1955–1963 period.

Historical lead (Pb) contaminations may also be used as chronostratigraphic markers in sediments (Renberg et al. 2001; Arnaud et al. 2004). Samples from core BLB0704 (1 cm sampling step) were analyzed for trace elements using conventional XRF method at the IFREMER marine geology laboratory of Brest. To disentangle natural and human-induced changes in Pb concentration, they were normalized to yttrium (Y), a lithophile element presenting comparable concentration and geochemical behaviour (Faure 1986).

Earthquakes can destabilize and trigger gravity-reworking of slope sediments in lacustrine basins (e.g. Doig 1990). This results in the deposition of particular layers which can be identified either in the central part of the basin or at the foot step of steep slopes. Linking such gravity-reworked sediment deposits with their respective potential triggering historical seismic event may thus yield additional chronological markers (Arnaud et al. 2002; Nomade et al. 2005; Chapron et al. 2007; Guyard et al. 2007). Historical earthquakes occurring over the last centuries in the region were all reported in the database of Lambert and Levret-Albaret (1996). The location of the epicentre and the Medvedev-Sponheuer-Karnik (MSK) intensity are filled for each earthquake. The MSK intensity denotes how strongly an earthquake affected a specific place based on the reported damage, allowing to assess the intensity of past events over the non-instrumental period. In order to apply this approach to the sediment record of Lake Blanc we used a method described by Lignier (2001) and subsequently used in Nomade et al. (2005). In a diagram of epicentre-lake distance vs. MSK intensity, epicentres of the major historic earthquakes (represented by points) and the regional seismic intensity propagation (represented by a line) are plotted. The seismic intensity propagation is constructed from two points: the distance to the epicentre of a well-known earthquake and the closest documented point to the lake affected by the same event. Keeping its slope this line is finally adjusted to the number of observed gravity-reworked sediment layers. The adjusted line corresponds to determine the sensitivity of study site in relation to earthquake intensity. This is the minimum seismic intensity causing a gravity-reworking of sediments. The resulting line permits thus to identify earthquakes which were theoretically close or strong enough to trigger gravity-reworking.

The direct downstream position of the village Sainte-Agnès and its abundant historic literature documenting floods events over the last ca. 200 years (Allignol et al. 2008) additionally allowed us to link high-magnitude flood events with particular sediment layers interpreted as flood deposits and add chronological markers similar to approaches described by Blass et al. (2003), Monecke et al. (2004) or Bøe et al. (2006).

4 Results

4.1 Sedimentology

All retrieved cores consist of fine-grained laminated sediments in which thicker (max. 1.5 cm) and coarser-grained layers (Fig. 2a) are interbedded. Three lithofacies were identified:

- Facies 1 consists of dark and light, sub millimetre-scale laminae, more or less discernable by eye, with a relative homogenous grain size (mean median grain size:

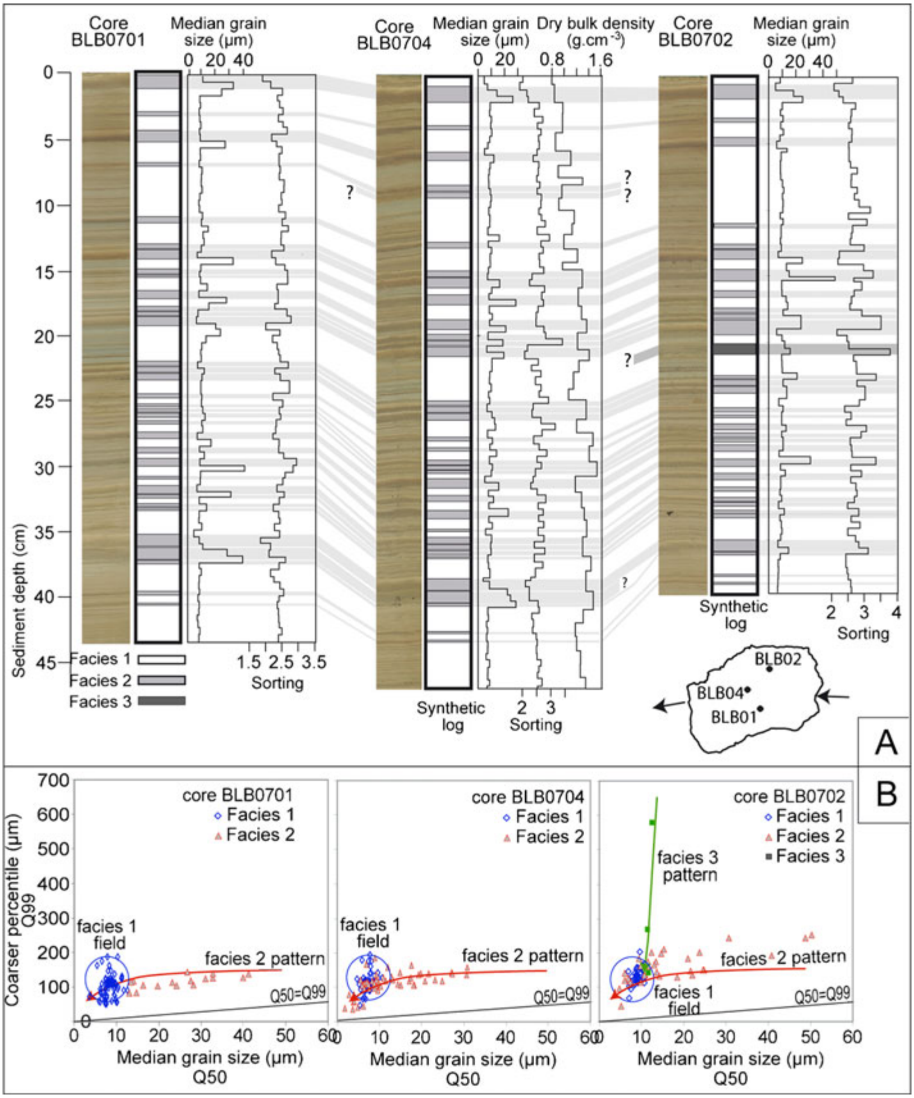

Fig 2 **a** Lithology, down core grain size characteristics of BLB0701, BLB0702 and BLB0704 and dry bulk density of BLB0704. **b** Q99 vs. Q50 plots of samples from the same cores

8.5 μm and mean sorting: 2.6 with standard deviation of 10.5% and 4.8%, respectively).

- Facies 2 is made of dark and thick layers, up to 1.5 cm, sometimes with a visible coarser basal part and always capped by a thin, whitish fine-grained layer. These layers are characterized by a fining upward sequence with a coarser median grain size at the base (27 to 37.7 μm, for cores BLB0704 and BLB0702, respectively) and a finer median grain size (6.9–7.3 μm) than other facies and a global mean sorting of 2.5 and 2.7.

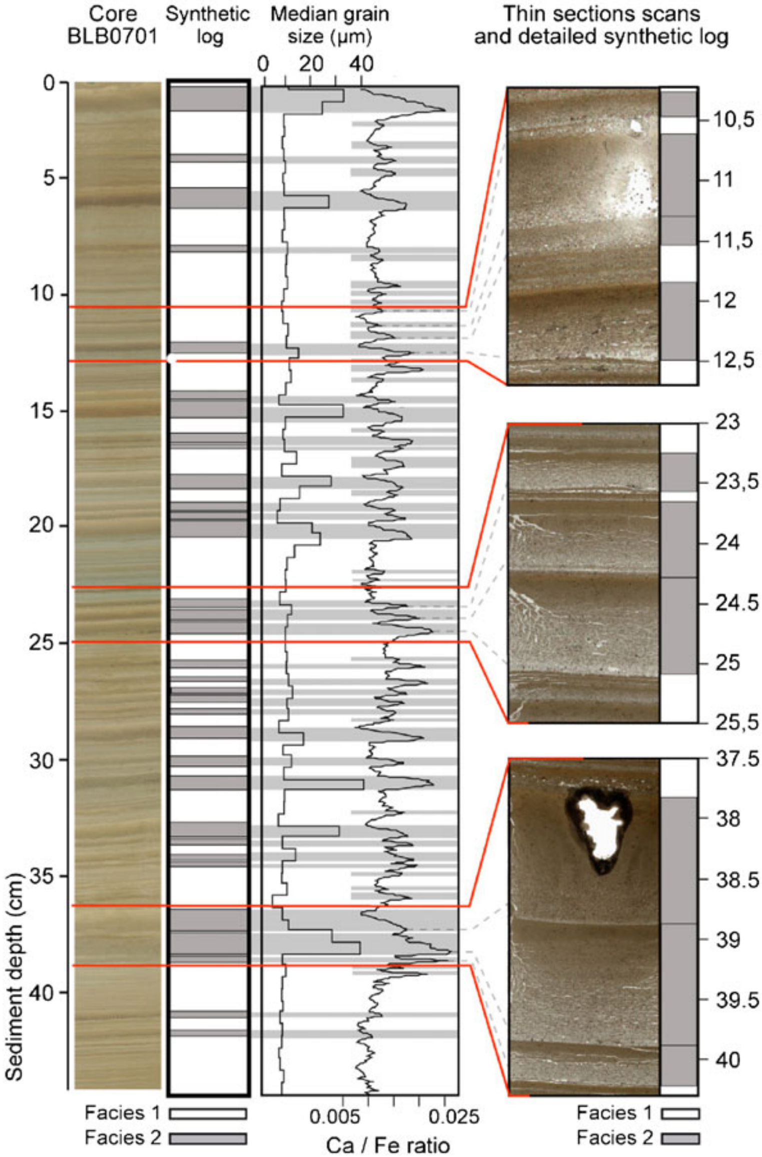

Fig. 3 Mean grain-size, raw 1-mm Ca/Fe ratio and scans of thin sections of the core BLB0701. Grey bars through the plots indicate event-triggered deposits determined by the both methods (for more explanation, see text). The hole in the lowest thin section resulted from an insufficient impregnation of the sediment

- Facies 3 is a centimetre-scale, sandy matrix-supported layer with a slightly coarser median grain size (12.3 μm) and a significantly higher mean sorting (3.01). This facies was found once, in core BLB0702.

In the diagram median (Q50) vs. coarser percentile (Q99), samples of facies 1 samples fall in a well-restrained field with a centre defined by a median (Q50) of 8 μm and a coarser percentile (Q99) of 120 μm (Fig. 2b). In contrast, facies 2 and 3 evolve two distinct dynamic patterns. Samples of facies 2 are close to the line Q50=Q99 which represents a perfect sorting while samples of facies 3 do not show any noticeable variations in the median grain size.

Microstratigraphic observations on thin sections allow a detailed comparison of grain size with the high-resolution Ca/Fe ratio to assess the pertinence of such a ratio as a grain size proxy (Fig. 3). Thin sections scans illustrate the macroscopically described interbedded layers, which are detected from the Ca/Fe ratio. In addition, layers which are too thin to be macroscopically identified, are found on both thin sections and in the Ca/Fe s. A significant correlation (r=0.76, n=20) was found between the median grain size and the 5 mm-resampled Ca/Fe signal for the thickest event-triggered deposits (Fig. 4). For the thinner ones (< 5 mm) no solid relationship was found owing to a dilution effect of the coarsest fraction with the facies 1 during the 5-mm sampling for conventional grain size analysis. Due its high resolution, the Ca/Fe ratio is therefore a more suitable grain size proxy than the classical grain size measurements in this detrital environment.

Finally the stratigraphic correlation of the interbedded layers between the four cores shows the presence of particular deposits only located in some parts of the lake basin (Fig. 2a). Facies 3 has only been observed in one layer in core BLB0702, taken at the foot of the steep northern slope. Furthermore, three distinctive layers of facies 2 are only present in cores BLB0701 and BLB0704 of the deepest part of the lake basin. Two of these layers are consecutive and well-distinguishable at about 8.5 and 9 cm in core BLB0704 but only one was found in the core BLB0701 at about 7 cm. The third layer was identified in cores BLB0701 and BLB0704 at 37.5 and 41 cm, respectively. There are thus altogether four distinctive interbedded layers localized just in some parts of the lake basin, one at the foot of a steep slope (facies 3) and three in the deepest part (facies 2).

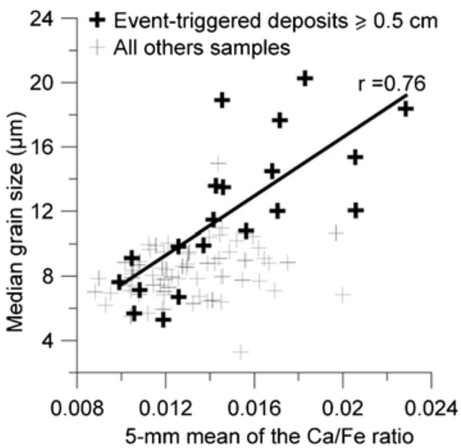

Fig. 4 Cross-plot of the median grain size vs. the 5 mm-resampled Ca/Fe signal from BLB0701 data and linear regression for samples of event-triggered deposits thicker than 5 mm

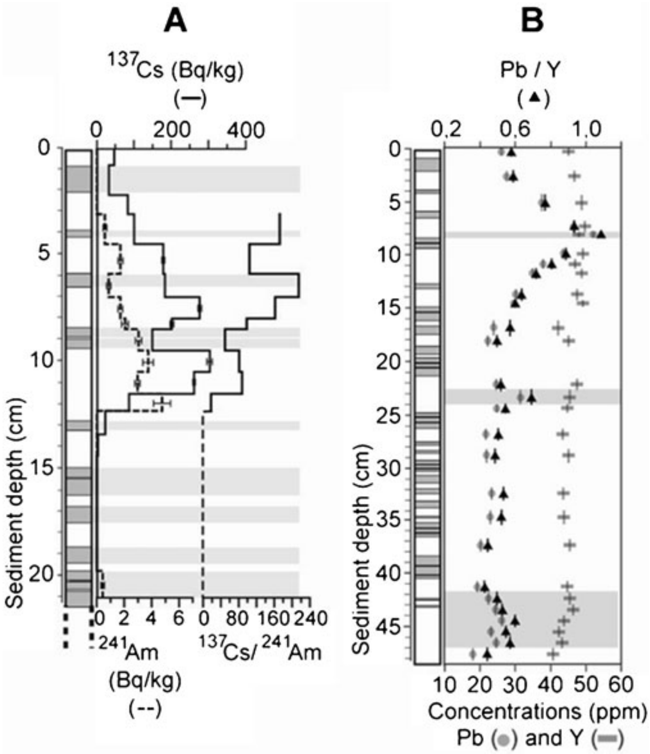

Fig. 5 Radionuclides and geochemical chronostratigraphic indicators from core BLB0704. **a** ^{137}Cs, ^{241}Am and ^{137}Cs/^{241}Am profiles. **b** Lead concentration profile, normalized by yttrium, permits to detect anthropogenic contamination (*shaded zones*)

4.2 Chronology

The ^{137}Cs record (Fig. 5a) shows a distinct increase of ^{137}Cs activities starting at about 13 cm and culminating with a first peak of more than 300 Bq/kg at 10 cm. A second peak occurs at 7.5 cm depth. The upper part of the profile from 0 to 7 cm is characterized by decreasing activity values. The deepest recorded ^{241}Am activity at 12 cm is also the highest one. Activities of ^{241}Am subsequently decrease towards the top with no detectable activities from 0 to 4 cm. The ^{137}Cs/^{241}Am profile shows a regular increase from 12 to 6 cm, disrupted by a sharp depletion at 9 cm corresponding to 2 large interbedded layers.

Values of yttrium (Y) are approximately constant along the core with a mean of 46 ppm and a standard deviation of 2.4% (Fig. 5b). The lead (Pb) profile has a base level of about 22 ppm with three important peaks. A first increase occurs at the base of the core at 42 to 47 cm sediment depth. A very sharp peak is found at 23–24 cm and a well-marked peak at 8 cm reaches the maximal value of 52 ppm.

Finally, earthquakes with an epicentral MSK intensity above V and a maximum distance of 110 km from the lake were carried forward in intensity vs. distance scatterplot (Fig. 6). The intensity propagation line was then constructed using the well-documented earthquake of Corrençon (AD 1962; Rothe 1972) with a recorded MSK intensity of VIII at the epicentre (38 km distance from the lake) and a MSK intensity of V at Sainte-Agnès which is

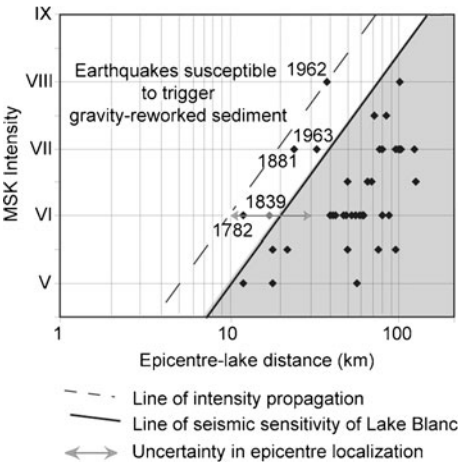

Fig. 6 Plot of historic earthquakes in the vicinity of Lake Blanc (MSK intensity>V and distance<110 km) in an intensity vs. distance diagram. The seismic sensitivity line permits to distinguish potential earthquakes susceptible to trigger gravity reworking from all historic earthquakes

the closest village from the lake at 5 km distance. By keeping its slope constant this line was then adjusted according to the number of recognized gravity-reworked sediment layers. The resulting line of seismic sensitivity separates potential seismic events which failed to leave an imprint in the sediment record from events triggering gravity-reworked layers, which now can be correlated to the known dates of the events.

5 Discussion

5.1 Triggering mechanisms of different sedimentary deposits

Differences in grain size patterns (Fig. 2a and b) lead to interpret different facies into three different depositional processes. The location of facies 1 in the Q50 vs. Q99 diagram indicates a "pelagic suspension" deposit pattern (Passega 1964). Facies 1 is thus due to the continuous deposit of regular stream inputs of glacial flour leading to the steady lake water turbidity.

The well-sorted facies 2 and the proximity between facies 2 pattern and the Q99=Q50 line (Fig. 2b) both suggest that these sediments were sorted by water currents (Passega 1964). Its fining-upward pattern mirrors a decreasing flow velocity during the flood event, whereas the thin whitish layer is due to the subsequent settling of finest particles (Arnaud et al. 2002). More over, the 15 m delta progradation (13.5% of the apex-shore distance, Fig. 1c) associated to the 2005 major flood, did affect the whole delta width. This implicates the river spreads over the whole delta during flood events and disperses the sediment over the whole lake basin. The grain size features and the spatial distribution of facies 2 layers are thus coherent, except for the three previously described layers only present in cores BLB0701 and BLB0704. Their grain size characteristics and limited spatial extensions in the deepest part of the lake basin suggest the occurrence of flow deposits originating from delta mass failure (e.g. Shiki et al. 2000).

Compared to facies 2, facies 3 is characterized by the absence of the clayey cap, poorer sediment sorting and a large variation of the Q99 parameter without noticeable Q50 variation. These latter observations confirm the optical description of a matrix-supported layer. This suggests the transport energy is supplied by sediment weight rather than by a water current velocity (Arnaud et al. 2002). It may thus be interpreted as a fluidized flow deposit (Mulder and Cochonat 1996) of reworked sediment from steep slopes surrounding BLB0702 coring site. Lacustrine gravity reworking may be attributed to spontaneous mass failure owing to sediment overloading, rockfall, snow avalanche, lake-level variation or local seismic activity (Monecke et al. 2004). Earthquakes or spontaneous failures seem to be the most probable triggering factors for Lake Blanc as other factors can be excluded for the study site.

XRF scanning data combined with macroscopic description and conventional grain size measurements led to establish a complete inventory of 56 flood deposits. Both the thickness and the accumulated sediment mass of each flood layer could potentially be used to assess the flood magnitude. As bulk density increase with depth (Fig. 2a) in the first 15 cm, sediment mass accumulation was preferred. In this aim accumulated mass per surface unit (g/cm^2) was assessed for each flood layer multiplying their thickness (cm) by their dry density (g/cm^3, Fig. 8a).

5.2 Chronology

5.2.1 Artificial radionuclides

According to ^{137}Cs and ^{241}Am profiles (Fig. 5), atmospheric nuclear tests fallout started at 13 cm depth (AD 1955) and culminated with the peak at 10 cm (AD 1963, UNSCEAR 2000). The sharp decrease above the peak probably corresponds either to the decrease of atmospheric nuclear tests from 1961 to 1962 to 1980, or to the reworking of older sediment. The uppermost activity peak of ^{137}Cs at 7.5 cm, can be attributed to Chernobyl accident (AD 1986). The highest value of $^{137}Cs/^{241}Am$ profile is located above the uppermost ^{137}Cs peak and corresponds to a deposit triggered by a flood which may have washed down and concentrated ^{137}Cs Chernobyl fallout.

5.2.2 Historical lead contaminations

Pb peaks are independent of the accumulation rate variations or rock weathering conditions, as shown by rather constant Y concentrations and can thus be interpreted as atmospheric anthropogenic contaminations. According to 137Cs, the uppermost peak is dated between AD 1963 and 1986 as inferred from the ^{137}Cs peaks (Fig. 5) and is likely related to the maximal use of leaded gasoline in 1973–1974 (e.g. Arnaud et al. 2004).

Older lead pollutions do not correspond to any well-known global contaminations in the literature. Their origin is therefore likely related to local pollution patterns. In the catchment area several old mining sites are known but neither their history nor period of functioning are well-constrained.

5.2.3 Identification of historical earthquakes

The four spatially-restricted deposits interpreted as gravity-reworked deposits, were potentially triggered by earthquake. From the distance-intensity plot (Fig. 6), five earthquakes can theoretically be considered to have triggered these four layers. According to Obermeier 1998; Lignier 2001; Monecke et al. 2004 and Nomade et al. 2005, all of them are in the range of intensity (VI–VIII) and distance from the lake (10–40 km) to be able to trigger gravity-reworking. However the earthquake in AD 1839 is uncertain because its epicentre is not clearly defined-between 10 and more than 30 km from the lake (Fig. 6), according to different sources (Rothe 1972). It was therefore not considered in the age-depth model. The two consecutive earthquake-triggered layers localized at 9 cm sediment depth in core BLB0704 can be dated to AD 1962 and AD 1963 which fits well with the ^{137}Cs peak of the atmospheric nuclear tests (Fig. 7). Finally the four earthquakes (AD 1782, 1881, 1962 and 1963) were already recognized as triggers of slope sediment destabilization in the nearby lakes Laffrey (Nomade et al. 2005), Blanc Huez (Guyard et al. 2007) and Bramant (Chapron et al. 2007).

5.2.4 Historical flood calendar

The uppermost flood layer is just below the sediment surface (Figs. 2 and 7) and is thus very likely due to the AD 2005 catastrophic flood event. Another large flood damaged the hydroelectric infrastructures and a road in the Vorz catchment in AD 1987. At Sainte-Agnès the discharge was similar as in 2005, but less solid material was mobilized during this event. A flood layer was identified at 6 cm depth in BLB0704 (Fig. 7) just above the Chernobyl ^{137}Cs peak and is thus attributable to the 1987 flood event.

To correlate older flood events and their corresponding deposits, we used the flood calendar derived from historical documents in local and departmental archives (Allignol et al. 2008). Twenty floods impacting the village of Sainte-Agnès are mentioned in these archives since AD 1748 among which fourteen ones concern the Vorz torrent (1831; 1851; 1852; 1852; 1906; 1912; 1924; 1933; 1939; 1948; 1987; 1991; 1998; 2005). We used the time constraints given by the historical earthquakes to assign these floods to their particular sedimentary counterparts. The five floods between AD 1906 and AD 1948 could correspond to the five flood deposits detected between the earthquakes of Allemond (AD 1881) and Corrençon-en-Vercors (AD 1962) (Fig. 7). The flood deposit associated with the AD 1948 event fits well with the beginning of the ^{137}Cs and ^{241}Am activities from the

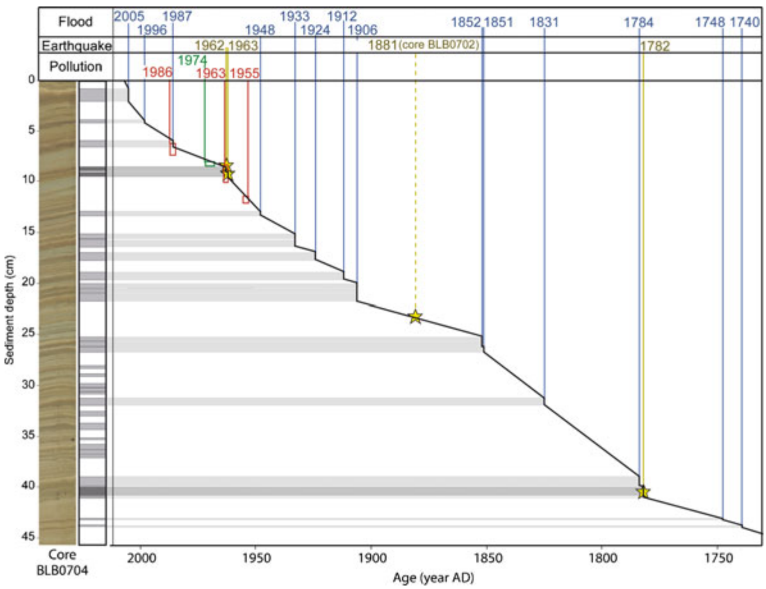

Fig. 7 Age-depth relationship for core BLB0704 established from detected periods of radioactive (*red*) and lead (*green*) global pollutions and historically documented earthquakes (*yellow*) and floods (*blue*). For explanation about origin of the dates, see the text

atmospheric nuclear tests (AD 1950). In the same way we associated the triplet of flood deposits located stratigraphically below the gravity-reworked deposit of "Allemond" (AD 1881) with the three successive historic flood events of AD 1851 and AD 1852 (two events in 1852). The date of AD 1831 was correlated with the last major flood deposit prior to this triplet. For the 18th century, local archives are very sparse and there is no flood date for the Vorz itself. The older proposed dates (AD 1740, 1748 and 1784) come from departmental archives and concern other rivers. The major flood event of 1784 happened just after the earthquake of 1782. This flood may thus be associated to the thick deposit directly above the earthquake-triggered deposit. However the absence of continuous sedimentation between both deposits suggests a very short time between the triggering events (< 1 year) or a sedimentary hiatus. Finally the dates of the two oldest events are based only on the extrapolation of the mean accumulation rate and remain thus uncertain.

Between dated flood deposits, mean sediment accumulation rates (between 0.4 and 2 cm/year for core BLB0701) were calculated in order to interpolate the age-depth model and to date flood layers which were not recorded in historic documents (Fig. 7). The assigned dates of these floods have an estimated uncertainty of some years (up to ±5 years).

5.3 Factors triggering floods

Flood-triggered deposits detected in Lake Blanc sediment record result from fast and large sediment input owing to exceptional high-magnitude river runoff events which erode, transport and spread the moraine material from the glacier foreland over the whole lake basin. The source of material on one hand and the triggering factors of high river discharge on the other hand are thus the keys for the understanding and the interpretation of the Vorz flood record.

5.3.1 Origin of the material

The main sediment source is the moraine complex mainly constructed by the three large glacier advances of the Little Ice Age (LIA) (Holzhauser et al. 2005). A vast quantity of easily erodible detrital matter is thus available since the beginning of the studied period. Basal till erosion may be more effective during periods of glacier retreats when the proglacial foreland is free of ice. However, only the lowest part of the proglacial area was affected by river erosion. Indeed main signs of active erosion observed in the field only concern the most distal moraine and in a less extent the basal till located just upstream (Fig. 1d). These observations suggest the possibility of moraine erosion even when the glacier was occupying its most distal positions at the end of the LIA. In addition basal till can also be eroded and transported by high-magnitude subglacial runoff events during these glacier phases (Benn and Evans 1998; Davies et al. 2003). The tongue of the Freydane glacier was relatively narrow in its lower and middle part owing to the valley morphology, suggesting a subglacial drainage system in dendritic channel network (Benn and Evans 1998). Reported travel times of melt water in this environment are less than 2 h for a distance of about 2 km (Nienow et al. 1998). During flood events the travel time of water from the catchment head to the lake and discharge at the outskirts of the proglacial area can thus be very similar when the glacier was in advanced positions or largely retreated as it is nowadays.

5.3.2 Flood typology and seasonality

In a small alpine catchment, high-magnitude runoff occurs only during high intensity precipitation event (Collins 1998; Merz and Blöschl 2003; Gaume et al. 2009). A neighbouring weather station was installed in 2003. It hence recorded the 2005 event: precipitations lasted mainly 2 days with daily rainfall amounts of respectively 174 and 126 mm (> 100-year return period, Gaume et al. 2009) and a maximum intensity reaching 9 mm/h. However, at the difference of this event, all other historic floods do not correspond to large scale catastrophes. Their high intensity and the fact they are isolated suggest Vorz flood events are usually triggered by local convective events ("Flash Floods" type from Merz and Blöschl 2003). This is confirmed by their seasonality: indeed, all of the documented historic floods occurred in summertime, when the occurrence of intense rainfall and convective events is the most probable (Kieffer-Weisse and Bois 2001; Merz and Blöschl 2003; Beniston 2006; Gaume et al. 2009).

5.4 Global climate context, frequency and magnitude of Vorz flood events

We documented 56 flood events in the Lake Blanc sediment sequence occurring from 1740 to 2007 (Fig. 8a). Our chronicle covers thus two distinct climatic periods; the end of the cold LIA (1740–1860) and the recent warming period (1860–2007).

5.4.1 Flood frequency

There is no distinction in flood occurrence between these two periods; 27 events (mean return period: 4.5 years) vs. 29 respectively (mean return period: 5 years). Three significant periods without any flood occurrence are noticeable: 1750–1775, during the L.I.A., 1870–1905 and 1960–1985 during the recent warming. Similarly periods of high flood frequency occurred during the LIA (1790–1805 and 1830–1845) as well as during the 20th century (1905–1915 and 1945–1960) with a similar frequency of 5–7 events per 11 years.

5.4.2 Flood intensity

The magnitude of the flood events was assessed from the quantity of material deposited per event. The most important deposits (~ 1 $g.cm^{-2}$) are consecutive and respectively associated to the 1782 historic earthquake and to the 1784 historic flood. The delta slope destabilisation following the earthquake may have disturbed the delta sedimentation pattern and resulted in a bias in the transported/deposited sediment during the "1784" flood event. The inferred magnitude of the "1784" flood event is thus associated with a high uncertainty. Others distinct flood deposits (> 0.8 $g.cm^{-2}$) were in decreasing order of magnitude (1784) 2005, 1906, 1987, 1933. All the strongest ones occurred thus during the recent warming period (20th century). Furthermore the 2005 flood event, felt by local residents to be an exceptional event, is indeed the strongest one (1 $g.cm^{-2}$) for at least the last two centuries or even maybe from the whole studied period. This result is supported by the observed delta progradation as well as the measured daily precipitation assessed to be much higher than the expected 100-year return period event (Gaume et al. 2009). Furthemore the flood of 1987 is assessed to be a catastrophic event (0.89 $g.cm^{-2}$) but less strong than the 2005 one, which is in agreement with the description of inhabitants.

5.5 Flood hazard evolution in the context of recent, current and future global climatic change

Flood events in the Vorz catchment are triggered by local, short but high intensity rainfalls. In the absence of long-term meteorological data from the catchment area, we use

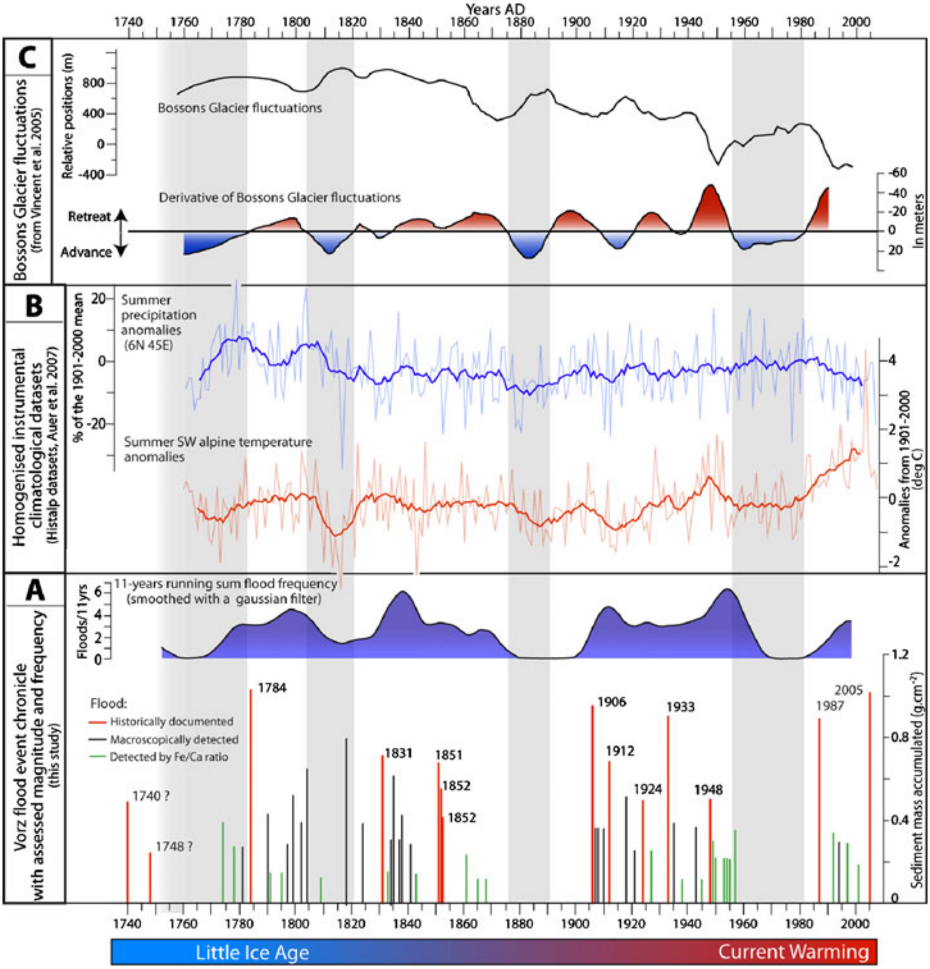

Fig. 8 Calendar of the 56 Vorz flood deposits, respective mass accumulated per event and flood frequency (**a**) compared with instrumental long series (**b**) and the fluctuations of the Glacier of Bossons (**c**). Each bar of the flood calendar represents one individual flood deposit and the size of the bar its deposit mass accumulated per unit of surface and per event, interpreted here as the magnitude of the flood event. The shaded zones correspond to the long-lasting periods of glacier advance

precipitation and temperature data derived from homogenised instrumental dataset covering almost the whole studied period (1760–2008) and the studied region (Histalp dataset; Auer et al. 2007). Monthly precipitation and temperature data permit to characterise climatic conditions favourable for triggering flood events. Summer dryness vs. wetness can be assessed from the mean June, July and August precipitations and temperature data (Fig. 8b). Furthermore glacier fluctuations are also shown as a high-elevation climate proxy (IPCC 2001). The glacier of Bossons (Mt. Blanc massif, ca. 100 km north-east from the study site) was chosen due to its fast response time to climate fluctuations. Glacier front variability shows two advances (1760–1780 and 1805–1820) before the large retreat initiated at the end of the LIA, punctuated by weaker advances (1875–1895 and 1950–1980; Fig. 8c, Vincent et al. 2005). The three periods without flood activity in Lake Blanc (1750–1775, 1870–1905 and 1960–1985) correspond to these advance phases. During the first part of the studied period the Freydane glacier reached the most distal LIA glacier position. The absence of flood activity during this phase could thus be interpreted as an effect of the extended ice cover. However, we argued previously that erosion of the basal till and the steep and most distal moraine was always possible whatever the position of the glacier tongue. Furthermore a comparable period without any flood event occurred in the 1960's when the glacier was largely retreated upstream the incised area. We thus interpret these contemporaneous phases of glacier advance and of reduced flood activity as distinct responses to a particular climate pattern characterised regionally by colder temperatures. Inversely periods of high flood frequency (1790–1805, 1830–1845, 1945–1960, 1905–1915, 1985–2007) seems to be associated with periods of higher temperatures. Among them, only the most recent one (1985–2007) was previously described in the region (Jomelli et al. 2007). The temperature-flood frequency relationship is based on the assumption that higher temperatures can theoretically trigger more high intensity rainfall (Trenberth 1999; Huntington 2006). However time-lags of 5 to 10 years are observed between warming and increase of flood frequencies, following the two very cold flood-free periods (1805–1820 and 1875–1890). This may be attributed to the time-lag necessary to thaw the periglacial permafrost which protects the moraine material from erosion as it has been documented in high elevation debris flow studies (e.g. Rebetz et al. 1997; Jomelli et al. 2007). According to the described altitudes (up to 2300–2400 m a.s.l.) of the current or past permafrost (Haeberli 1975; Rebetz et al. 1997; Jomelli et al. 2007) the proglacial area might have been affected by the permafrost during these extreme periods. In the recent period of global warming some studies report a decrease of total rainfall amounts but with higher intense events (e.g. Beniston et al. 1997; Frei and Schär 2001). Summer precipitation and Vorz floods triggered by high intensity events were compared trying to evidence such a relationship. However summer precipitations show no significant relation with the flood frequency and/or magnitude (Fig. 8).

6 Conclusion

Our study of lacustrine sediments permitted us to reconstruct a detailed flood calendar for the last 270 years based on independent dating methods. The magnitude of each event has been assessed from the quantity of material deposited per event in the lake. The obtained flood calendar reports 56 floods over the last 270 years with an assessed magnitude ranging from 0.1 to 1.1 g.cm^{-2}. Only 17 of these floods are mentioned in historical documents with no unbiased indication of their magnitude. The paleolimnological approach appears thus as an excellent way to assess both frequency and magnitude of flash flood activity in mountainous regions where instrumental records are rare and extreme precipitation patterns can only poorly be modelled.

The comparison of the obtained flood calendar with alpine temperature and precipitation data as well as glacier fluctuations suggests a relationship between climatic change and the evolution of torrential activity. No relationship was found with long-term precipitation records but a complex relationship with temperature seems to exist. No general trend appears between the end of the LIA and the 20th century but the flood frequency increases on a decadal timescale during warming periods, whereas virtually no floods are recorded during glacier advances. After the coldest periods time-lag of flood activity increase occurred, suggesting the temporary presence of permafrost conditions. This could have weakened the efficiency of erosion processes during high precipitation events. We showed that the probability of occurrence for extreme flood events increased with a long term temperature rise. Among the 7 extreme flood events, 4 ones occurred during the 20th century, but they are ranked as the most extreme ones. In particular, the 2005 event is the strongest of the whole considered period. These results support the hypothesis of an increase of heavy rainfall events due to the enhancement of the hydrologic cycle in the context of global warming.

The presented results are representative of a relatively small area and therefore give only a local signal of precipitation changes. In order to obtain a more regional climate evolution, several other lakes are currently studied. These data will improve and constrain our understanding of the relationship between climatic change and devastating flood events.

Acknowledgments B. Wilhelm's work is supported by a grant from the Assemblée des Pays de Savoie and the Communauté de Communes des Balcons de Belledonne. Logistical and financial supports were brought in the framework of the scientific programmes Vorz, founded by the Communauté de Communes des Balcons de Belledonne and Pygmalion, founded by the French National Research Agency (ANR BLAN07-2_204489). Authors are particularly grateful to the Sainte Agnes' mayor who launched the Vorz programme and brought valuable help for field campaigns. Authors are grateful to Prof. Bernd Zolitschka who kindly permitted the access to the Geopolar XRF core scanner device and to the database Histalp which permits to obtain free climatological long series (http://www.zamg.ac.at/histalp). Thin sections were performed thanks to the technical facilities of the "plateforme d'analyses structurales et environnementales" (ASTRE) of the University of Savoie. Finally authors are grateful to the four anonymous reviewers for their helpful comments.

References

Allignol F, Arnaud F, Champagnac J.D, Delannoy JJ, Deline P, Fudral S, Paillet A, Ployon E, Ravanel L, Saulnier GM, Wilhelm B (2008) Etude intégrée du bassin versant du Vorz (Belledonne, Isère) consécutive à la crue des 22 et 23 août 2005. Rapport scientifique, Laboratoire EDYTEM, Le Bourget du Lac, p. 202

Appleby PG, Richardson N, Nolan PJ (1991) 241Am dating of lake sediments. Hydrobiol 214:35–42

Arnaud F, Lignier V, Revel M, Desmet M, Pourchet M, Beck C, Charlet F, Trentesaux A, Tribovillard N (2002) Flood and earthquake disturbance of 210Pb geochronology (Lake Anterne, North French Alps). Terra Nova 14:225–232

Arnaud F, Revel-Rolland M, Winiarski T, Chapron E, Desmet M, Tribovillard N, Givelet N (2004) History of lead contamination in Northern French Alps from distant lake sediment records. J Environ Monit 6:448–456

Auer I, Böhm R, Jukovic A, Lipa W, Orlik A, Potzmann R, Schöner W, Ungersböck M, Matulla C, Briffa K, Jones P, Efthymiadis D, Brunetti M, Nanni T, Maugeri M, Mercalli L, Mestre O, Moisselin JM, Begert M, Müller-Westermeier G, Kveton V, Bochnicek O, Stasny P, Lapin M, Szalai S, Szentimrey T, Szentimrey T, Cengar T, Dolinar M, Gajic-Capka M, Zaninovic K, Majstorovicp Z, Nieplovaq E (2007) HISTALP – historical instrumental climatological surface time series of the Greater Alpine Region. Int J Climatol 27:17–46

Beniston M (2006) August 2005 intense rainfall event in Switzerland: not necessarily an analog for strong convective events in a greenhouse climate. Geophys Res Lett 33:L05701

Beniston M, Stephenson DB (2004) Extreme climatic events and their evolution under changing climatic conditions. Glob Planet Change 44:1–9

Beniston M, Diaz HF, Bradley RS (1997) Climatic change at high elevation sites: an overview. Clim Change 36:233–251

Benito G, Lang M, Barriendos M, Llasat MC, Francés F, Ouarda T, Thorndycraft VR, Enzel Y, Bardossy A, Coeur D, Bobée B (2004) Use of Systematic, palaeoflood and historical data for the improvement of flood risk estimation, review of scientific methods. Nat Hazards 3:623–643

Benn DI, Evans DJA (1998) Glaciers and glaciation. Edward Arnold, London, 734

Blass A, Anselmetti FS, Ariztegui D (2003) 60 years of glaciolacustrine sedimentation in Steinsee (Sustenpass, Switzerland) compared with historic events and instrumental meteorological data. Eclogae Geol Helv 96(1):59–71

Bøe AG, Olaf Dahl S, Lie O, Nesje A (2006) Holocene river floods in the upper Glomma catchment, southern Norway: a high-resolution multiproxy record from lacustrine sediments. Holocene 16(3):445–455

Böhm O, Wetzel KF (2006) Flood history of the Danube tributaries Lech and Isar in the Alpine foreland of Germany. Hydrol Sci J 51(5):784–798

Brazdil R, Pfister C, Wanner H, Von Storch H, Luterbacher JR (2005) Historical climatology in Europe—the state of the art. Clim change 70:363–430

Bronstert A (2003) Floods and climate change: interactions and impacts. Risk Anal 23(3):545–557

Chapron E, Beck C, Pourchet M, Deconinck JF (1999) 1822 earthquake-triggered homogenite in Lake Le Bourget (NW Alps). Terra Nova 1:86–92

Chapron E, Faïn X, Magand O, Charlet L, Debret M, Mélières MA (2007) Reconstructing recent environmental changes from proglacial lake sediments in the Western Alps (Lake Blanc Huez, 2543 ma. s.l., Grandes Rousses Massif, France). Palaeogeogr Palaeoclimatol Palaeoecol 252:586–600

Collins D (1998) Rainfall-induced high-magnitude runoff events in highly-glacierized Alpine basins. Hydrol, Water Resour Ecol in Headwaters. IAHS Publ 248:69–78

Cuven S, Francus P, Lamoureux S (2010) Estimation of grain size variability with micro X-ray fluorescence in laminated lacustrine sediments, Cape Bounty, Canadian High Arctic. J Paleolimnol 44(3):803–817

Davies TRH, Smart CC, Turnbull JM (2003) Water and sediment outbursts from advanced Franz Joseg glacier, New Zealand. Earth Surf Process Landforms 28:1081–1096

Di Lauro A, Fernex F, Fierro G, Ferrand JL, Pupin JP, Gasparro J (2004) Geochemical approach to the sedimentary evolution of the Bay of Nice (NW Mediterranean sea). Cont Shelf Res 24:223–239

Doig R (1990) 2300 yr history of seismicity from silting events, in Lake Tadoussac, Charlevoix, Quebec. Geology 18(9):820–823

Edouard JL (1994) Les lacs d'altitude dans les Alpes françaises, contribution à la connaissance des lacs d'altitude et à l'histore des milieux montagnards depuis la fin du Tardiglaciaire. Thèse soutenue à l'University J. Fourier de Grenoble

Faure G (1986) Principles of isotope geology. Wiley, New York, p 286

Frei C, Schär C (2001) Detection probability of trends in rare events: theory and application to heavy precipitation in the alpine region. J Clim 14:1568–1584

Frei C, Schöll R, Fukutome S, Schmidli J, Vidale PL (2006) Future change of precipitation extremes in Europe: Intercomparison of scenarios from regional climate models. J Geophys Res-Atm 111:D06105. doi:10.1029/2005JD005965

Gaume E, Bain V, Bernardara P, Newinger O, Barbuc M, Bateman A, Blaškovičová L, Blöschl G, Borga M, Dumitrescu A, Daliakopoulos I, Garcia J, Irimescu A, Kohnova S, Koutroulis A, Marchi L, Matreata S, Medina V, Preciso E, Sempere-Torres D, Stancalie G, Szolgay J, Tsanis I, Velasco D, Viglione A (2009) A compilation of data on European flash floods. J Hydrol 367:70–78

Giguet-Covex C, Arnaud F, Poulenard J, Disnar JR, Delhon C, Francus P, David F, Enters D, Rey PJ, Delannoy JJ (2011) Changes in erosion patterns during the Holocene in a currently treeless subalpine catchment inferred from lake sediment geochemistry (Lake Anterne, 2063 m asl, NW French Alps): the role of climate and human activities. Holocene. doi:10.1177/0959683610391320

Gilli A, Anselmetti FS, Ariztegui D, McKenzie JA (2003) A 600-year sedimentary record of flood events from two sub-alpine lakes (Schwendiseen, Northeastern Switzerland). Eclogae Geol Helv 96(1):49–58

Grieser J, Beck C, Rudolf B (2005) The summer flooding 2005 in Southern Bavaria – a climatological review. Klimastatusbericht 2005:168–173

Guyard H, Chapron E, St-Onge G, Anselmetti FS, Arnaud F, Magand O, Francus P, Melières MA (2007) High-altitude varve records of abrupt environmental changes and mining activity over the last 4000 years in the Western French Alps (Lake Bramant, Grandes Rousses Massif). Quat Sci Rev 26:2644–2660

Haeberli W (1975) Untersuchungen zur Verbreitung von Parmafrost zwischen Flüelapass und Piz Grialetsch (Graubünden). *Mitteilung der Versuchsanstalt für Wasserbau, Hydrologie und Glaziologie an der Eidgenössischen Technischen Hochschule Zürich*, 17, 221 p.

Holzhauser H, Magny M, Zumbühl HJ (2005) Glacier and lake-level variations in west-central Europe over the last 3500 years. Holocene 15(6):789–801

Huntington TG (2006) Evidence for intensification of the global water cycle: Review and synthesis. J Hydrol 319:83–95

Intergovernmental Panel on Climate Change (2001) Climate change: contribution of working group i to the third assessment report of the intergovernmental panel on climate change. Cambridge Univ. Press, New York

Irmler R, Daut G, Mäusbacher R (2006) A debris flow calendar derived from sediments of lake Lago di Braies (N. Italy). Geomorphol 77:69–78

Jasper K, Gurtz J, Lang H (2002) Advanced flood forecasting in Alpine watersheds by coupling meteorological observations and forecasts with a distributed hydrological model. J Hydrol 267:40–52

Jaun S, Ahrens B, Walser A, Ewen T, Schär T (2008) A probabilistic view on the August 2005 floods in the upper Rhine Catchment. Nat Hazards Earth Syst Sci 8:281–291

Jomelli V, Brunstein D, Grancher D, Pech P (2007) Is the response of hill slope debris flows to recent climate change univocal? A case study in the Massif des Ecrins (French Alps). Clim Change 85:119–137
Karl TR, Trenberth KE (2003) Modern global climate change. Sci 302:1719–1723
Kieffer-Weisse A, Bois P (2001) Estimation de paramètres statistiques des précipitations extrêmes dans les Alpes françaises. La Houille Blanche 1:62–70
Lambert J, Levret-Albaret A (1996) Mille ans de séismes en France. Ouest Editions, Nantes, p 79
Lignier V (2001) Les sédiments lacustres et l'enregistrements de la paléosismicité, étude comparative de différents cas dans le Quaternaire des Alpes Nord-Occidentales et du Tien-Shan Kyrghyze. Thèse soutenue à l'University de Savoie
Lotter AF, Lemcke G (1999) Methods for preparing and counting biochemical varves. Boreas 28(2):243–252
Merz R, Blöschl G (2003) Regional flood risk—what are the driving processes? Water Resour Syst- Hydrol Risk, Manag Dev IAHS Publ 281:49–58
Milly PCD, Wetherald RT, Dunne KA, Delworth TL (2002) Increasing risk of great floods in a changing climate. Nat 415:514–517
Monecke K, Anselmetti FS, Becker A, Sturm M, Giardini D (2004) The record of historic earthquakes in lake sediments of Central Switzerlanc. Tectonophysics 394:21–40
Moreno A, Valero-Garcés BL, Gonzales-Sampériz P, Rico M (2008) Flood response to rainfall variability during the last 2000 years inferred from the Taravilla Lake record (Central Iberian Range, Spain). J Paleolimnol 40:943–961
Mulder T, Cochonat P (1996) Clasification of offshore mass movements. J Sedimentol Res 66(1):43–57
Nesje A, Olaf Dahl S, Matthews JA, Berrisdorf MS (2001) A 4500 years of river floods obtained from a sediment core in Lake Atnsjoen, eastern Norway. J Paleolimnol 25:329–342
Nienow P, Sharp M, Willis I (1998) Seasonal changes in the morphology of the subglacial drainage system, Haut Glacier d'Arolla, Switzerland. Earth Surf Process Landforms 23:825–843
Nomade J, Chapron E, Desmet M, Reyss JL, Arnaud F, Lignier V (2005) Reconstructing historical seismicity from lake sediments (Lake Laffrey, Western Alps, France). Terra Nova 17:350–357
Obermeier SF (1998) Liquefaction evidence for strong earthquakes of Holocene and latest Pleistocene ages in the states of Indiana and Illinois, USA. Eng Geol 50:227–254
Passega R (1964) Grain-size representation by CM patterns as a geological tool. J Sediment Petrol 34 (4):830–847
Prudent-Richard G, Gillet M, Vengeon JM, Descotes-Genon S (2008) Changements climatiques dans les Alpes : Impacts et risques naturels. Rapport Technique de l'O.N.E.R.C., p. 99
Rebetz M, Lugon R, Baeriswyl PA (1997) Climatic change and debris flows in high mountain regions: the case study of the Ritigraben Torrent (Swiss Alps). Clim Change 36:371–389
Renberg I, Bindler R, Bränvall ML (2001) Using the historical atmospheric lead-deposition record as a chronological marker in sediment deposits in Europe. Holocene 11(5):511–516
Rothe E (1972) Annales de l'Institut de Physique du Globe, 3e Partie géophysique. T. IX, University Louis Pasteur, 134
Shiki T, Kumon F, Inouchi Y, Kontani Y, Sakamoto T, Tateishi M, Matsubara H, Fukuyama K (2000) Sedimentary features of the seismo-turbidites, Lake Biwa, Japan. Sediment Geol 135:37–50
Siegenthaler C, Sturm M (1991) Die Häufigkeit von Ablagerungen extremer Reuss-Hochwasser. Die Sedimentationsgeschichte im Urnersee seit dem Mittelalter, In: Ursachenanalyse der Hochwasser 1987. Ergebnisse der Untersuchungen. Mitteilungen des Bundesamtes für Wasserwirtschaft 4:127–139
Trenberth KE (1999) Conceptual framework for changes of extremes of the hydrological cycle with climate change. Clim Change 42:327–339
UNSCEAR (2000) United Nations Scientific Committee on the Effects of Atomic Radiation, Sources and Effects of Ionizing Radiation. In: Report to the General Assembly (ed) United Nations, New-York, Annex C, exposures to the public from man-made sources of radiation, pp 158–291
Vincent C, Le Meur E, Six D, Funk M (2005) Solving the paradox of the end of the Little Ice Age in the Alps. Geophys Res Lett 32:L09706. doi:10.1029/2005GL022552